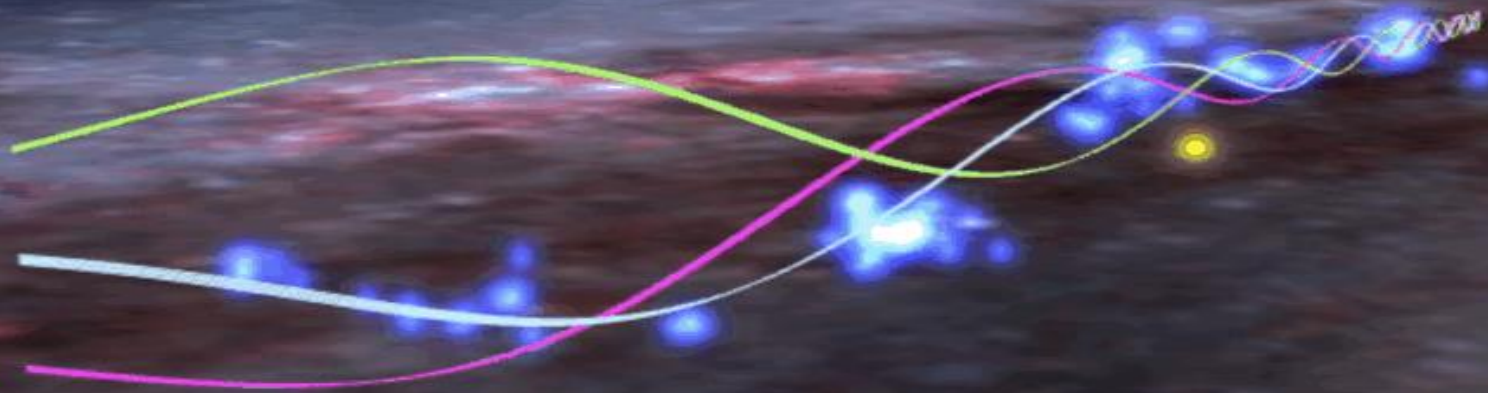


Open clusters in the Radcliffe Wave



Javier Alonso Santiago
(INAF – OA Catania)

THE RADCLIFFE WAVE



THE RADCLIFFE WAVE

~~Gould Belt ??~~

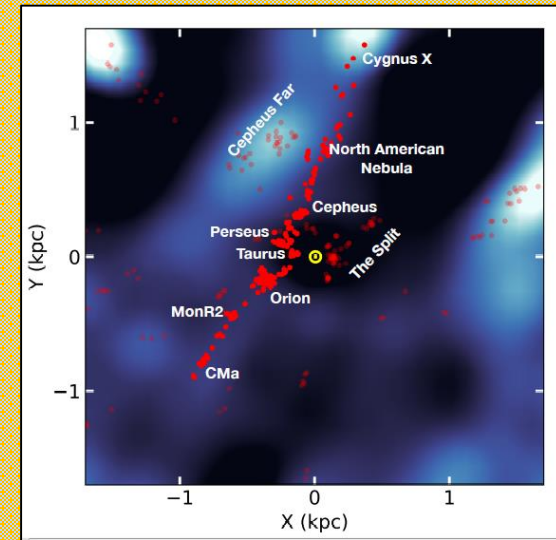
New vision of the Local ISM



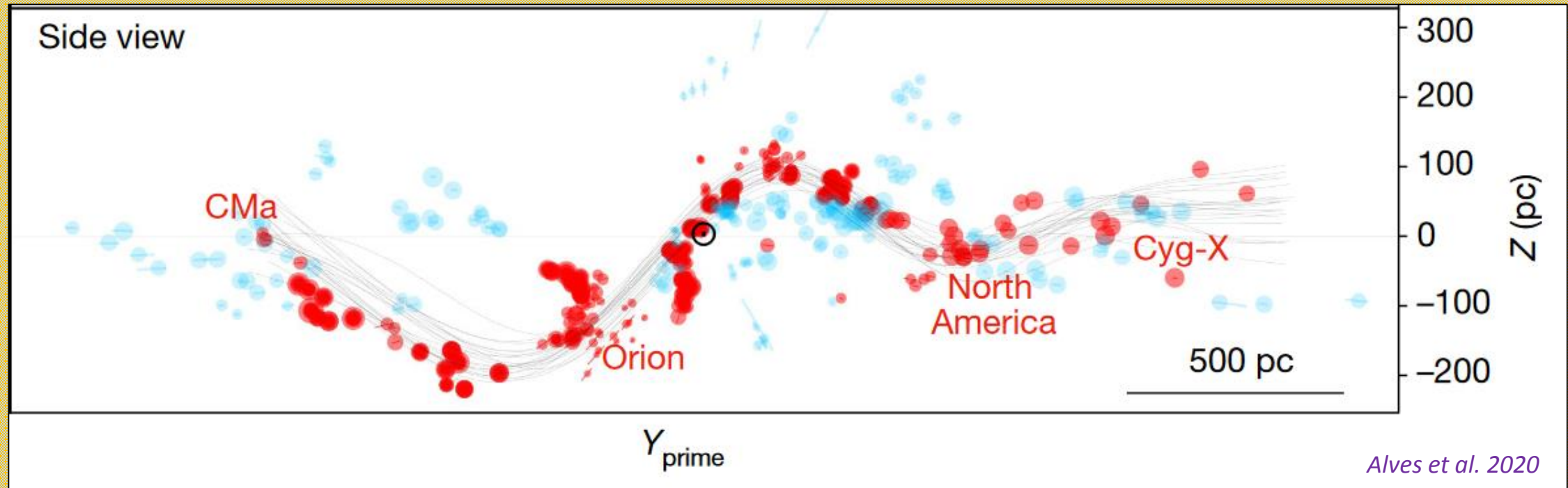
THE RADCLIFFE WAVE

“A Galactic-scale gas wave in the solar neighbourhood”

Alves et al. 2020



Swiggum et al. 2022

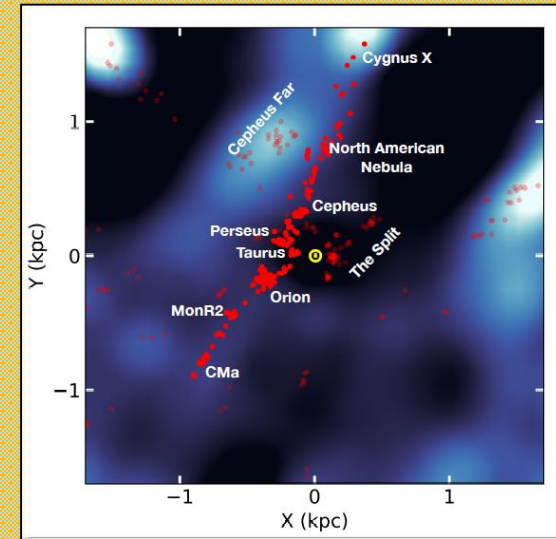


Alves et al. 2020

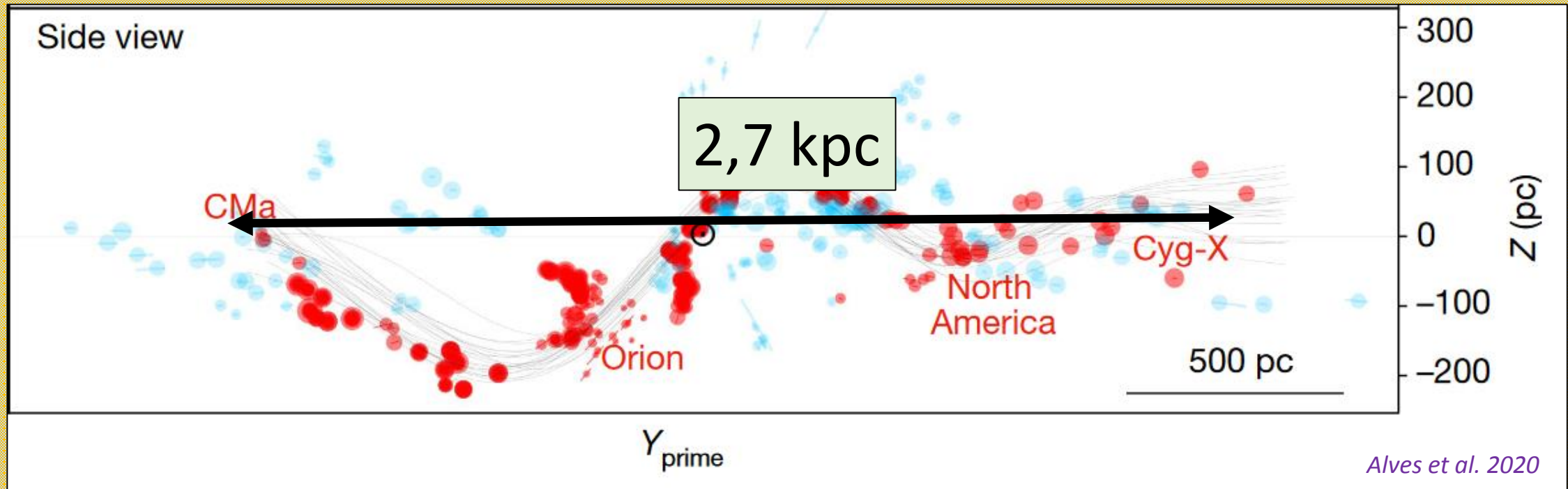
THE RADCLIFFE WAVE

“A Galactic-scale gas wave in the solar neighbourhood”

Alves et al. 2020



Swiggum et al. 2022

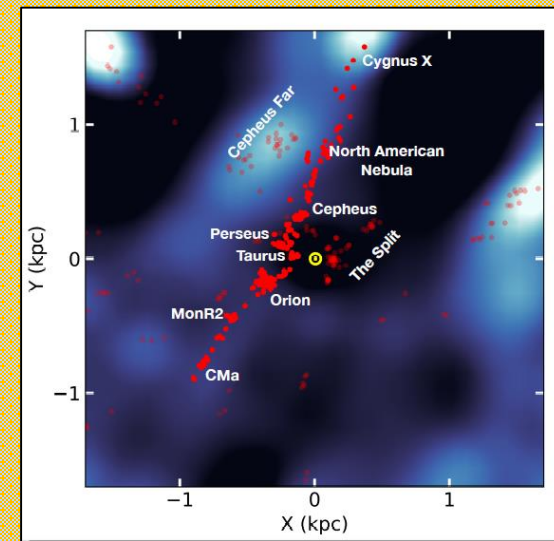


Alves et al. 2020

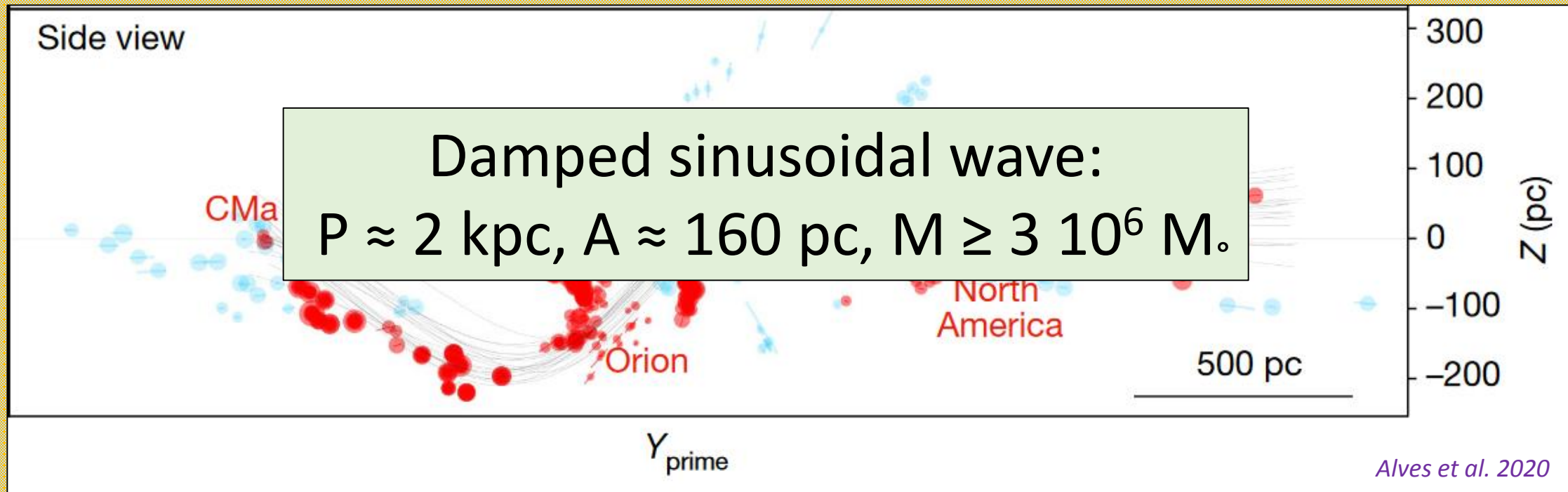
THE RADCLIFFE WAVE

“A Galactic-scale gas wave in the solar neighbourhood”

Alves et al. 2020

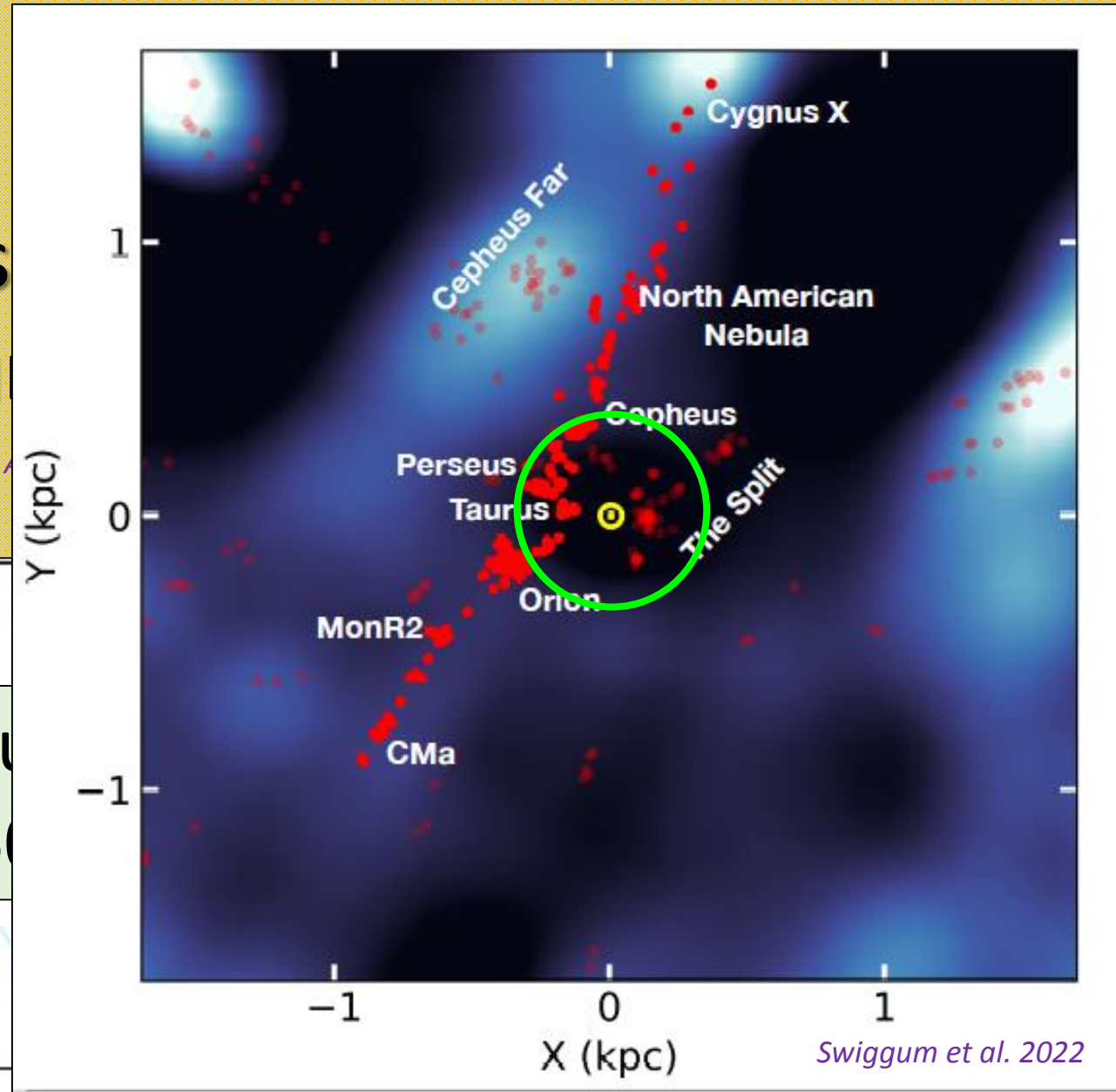
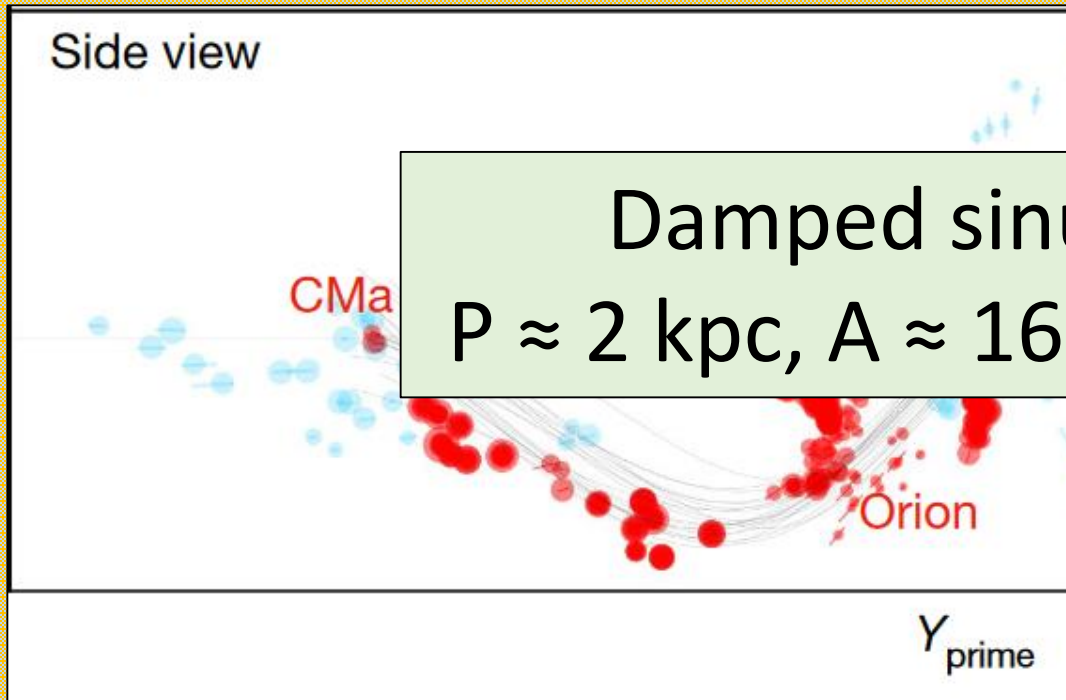


Swiggum et al. 2022



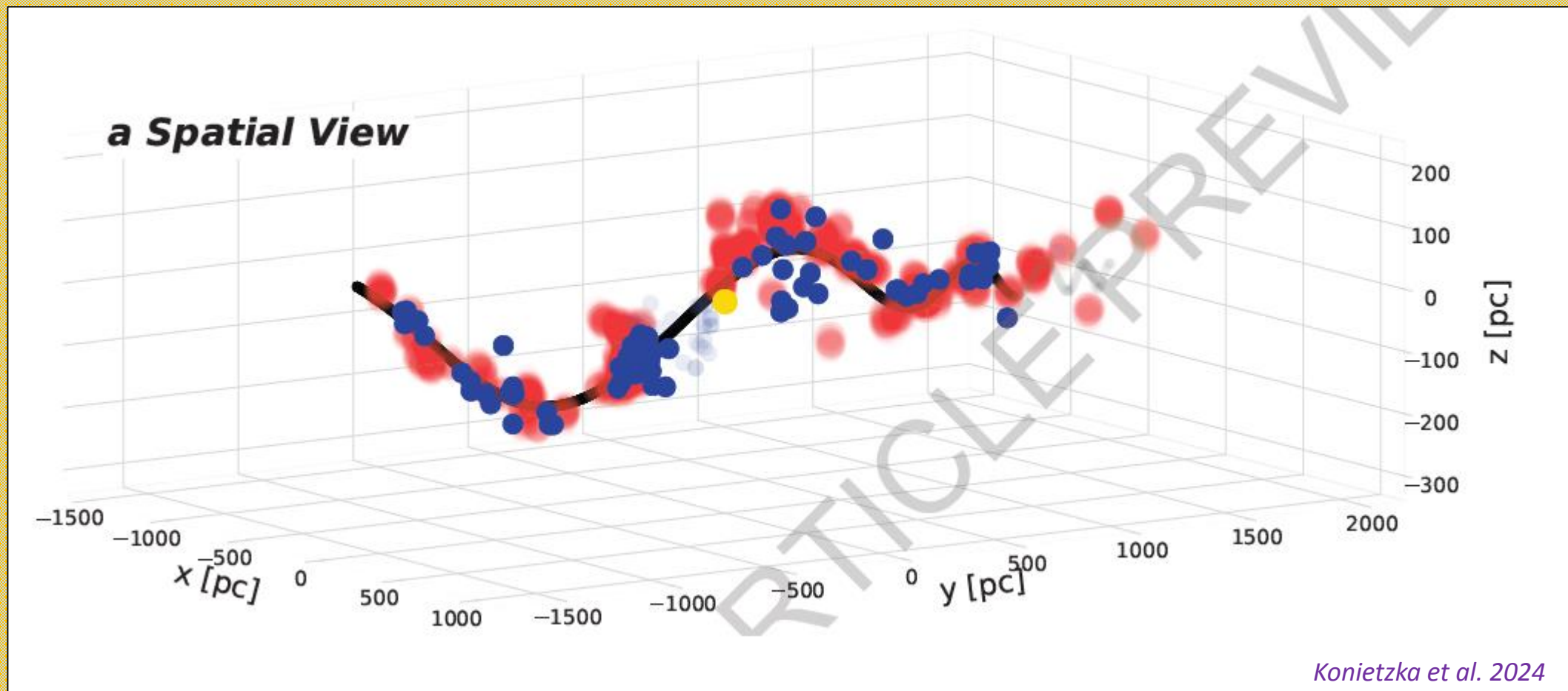
THE RADCLIFFE WAVE

“A Galactic-scale gas wave in the solar neighbourhood”



THE RADCLIFFE WAVE

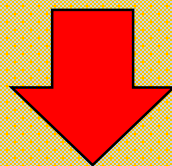
“The Radcliffe Wave is Oscillating”



THE RADCLIFFE WAVE

What about its chemical composition?

The Wave and its individual complexes, a natural laboratory



Star formation in giant molecular clouds, metal mixing?

INAF – TIME ALLOCATION COMMITTEE

Application for observing time

Category: D

Period AOT46 (October 2022 – March 2023)

Submit using: www.tng.iac.es/submit.html

1. Title

Metal mixing in the Radcliffe Wave traced by young open clusters

2. Abstract

The Radcliffe Wave has only recently been recognised as a ~ 3 kpc long coherent gas structure encompassing the majority of star forming regions in the solar vicinity. Also young (age ≤ 100 Myr) open clusters have been tentatively associated to the Radcliffe Wave. A dynamical connection between the regions along the Wave remains elusive and the nature and origin of this feature found in the dense gas are not well understood. Measuring stellar detailed chemical composition is in principle easier than determining information from the molecular gas. We propose to use GIARPS observations to derive detailed chemical abundances and radial velocities for 25 stars in five young clusters associated to the Wave to derive further insight about its history. By observing open clusters at different positions along the Radcliffe Wave we will provide useful constraints on the possible differences, which could be related to inhomogeneous mixing in the natal clouds. The chemical characterisation will mainly rest on HARPS-N spectra. GIANO spectra, besides providing more information for elements of interest (e.g., O, C, Zn), have the unique bonus of measurement of the helium abundance.

3a. Number of requested hours per telescope and instrument (must include overheads)

TNG						REM	
DOLORES	DOL.+MOS	NICS	HARPS-N	GIANO-B	SIFAP2	ROSS	REMIR
			31.3	31.3			

3b. Observing modes

TNG:	<input checked="" type="checkbox"/> Visitor	<input type="checkbox"/> Service	<input type="checkbox"/> ToO
REM:	<input type="checkbox"/> Rapid Response	<input type="checkbox"/> Queuing	<input type="checkbox"/> ToO

4a. Preferred months

first choice: October second choice: Sep, Nov

4b. Other scheduling constraints (use also box 14)

These observations will be performed in GIARPS mode.

5a. Past and future of the project

a) Hours already awarded to the project: 0

b) Hours foreseen to complete the project: 0
(not including this request)

6. Principal investigator

Name **Angela Bragaglia**

Institute INAF-OAS Bologna

Address via P. Gobetti 93/3, 40129 Bologna

e-mail angela.bragaglia@inaf.it

Phone +390516357332

7. Co-investigators (name and institution)

-Javier Alonso-Santiago, Giovanni Catanzaro, Antonio Frasca: INAF-OA Catania, Italy

-Gloria Andreuzzi: INAF-OA Roma, Italy;
Fundacion Galileo Galilei, Spain

-Ricardo Carrera, Valentina D'Orazi, Sara Lucatello, Lorenzo Spina, Antonella Vallenari: INAF-OA Padova, Italy

-Laura Magrini: INAF-OA Arcetri, Italy

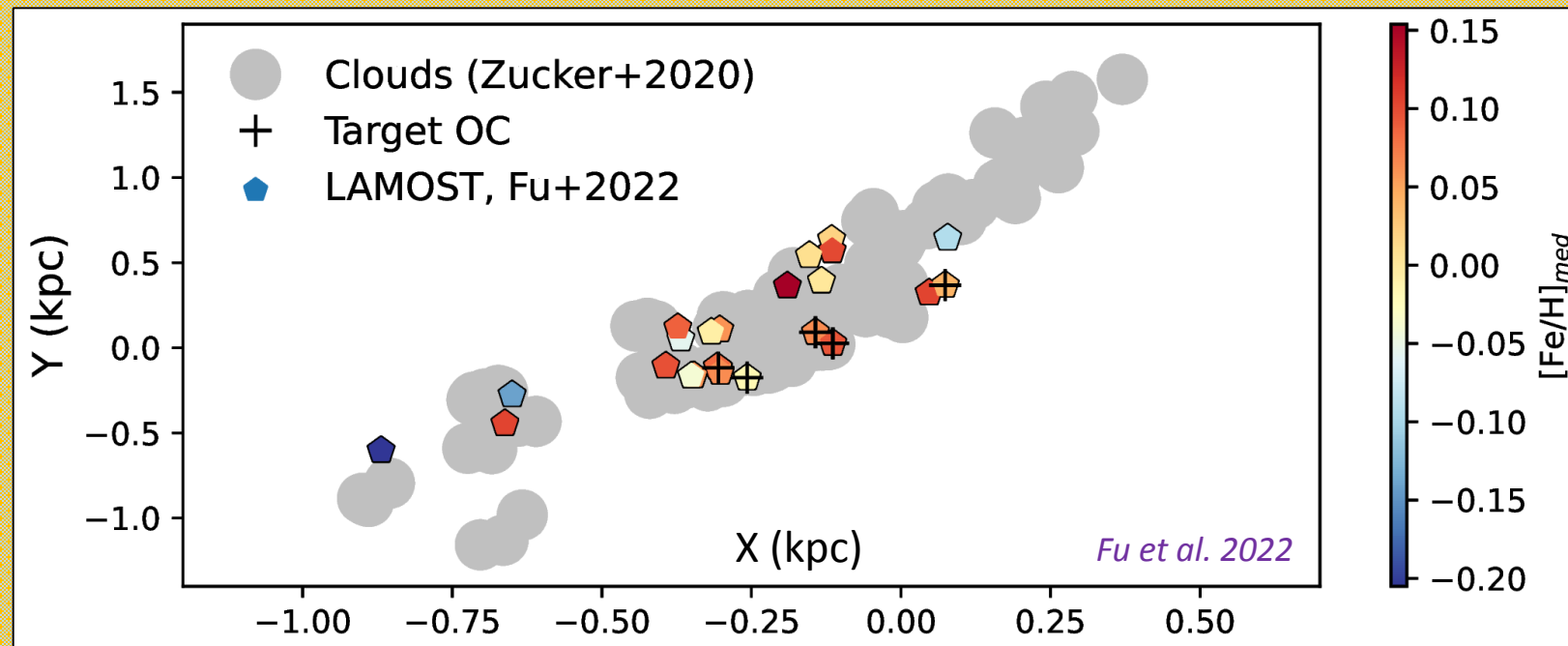
-Xiaoting Fu: Peking University, China (& INAF-OAS Bologna associate)

-Mingjie Jian: Tokyo University, Japan

TARGET SELECTION

1 – SAMPLE OF **OPEN CLUSTERS** ASSOCIATED WITH THE RADCLIFFE WAVE

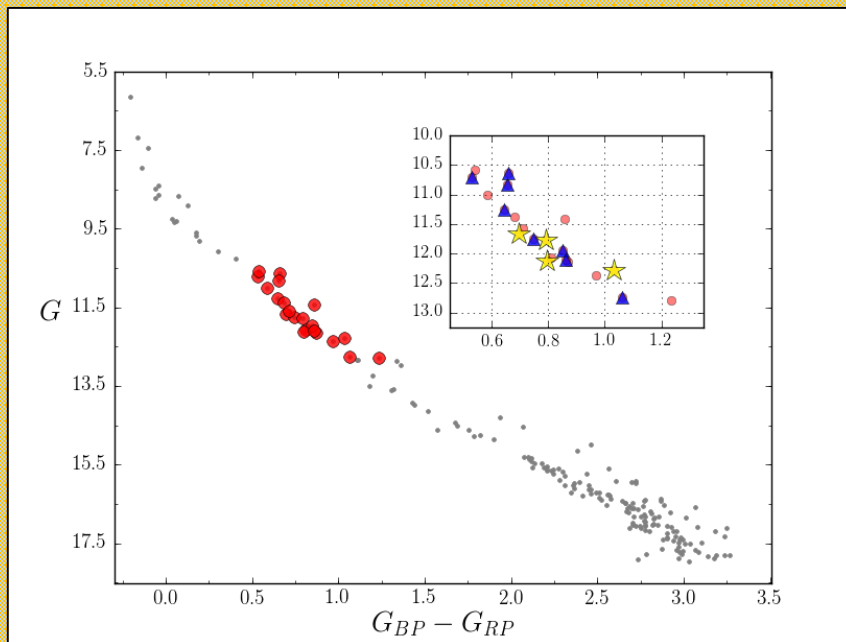
ASCC 16, NGC 2232, Roslund 6 + Pleiades, Melotte20



TARGET SELECTION

2 – SELECTION OF **INDIVIDUAL STARS** IN EACH CLUSTER

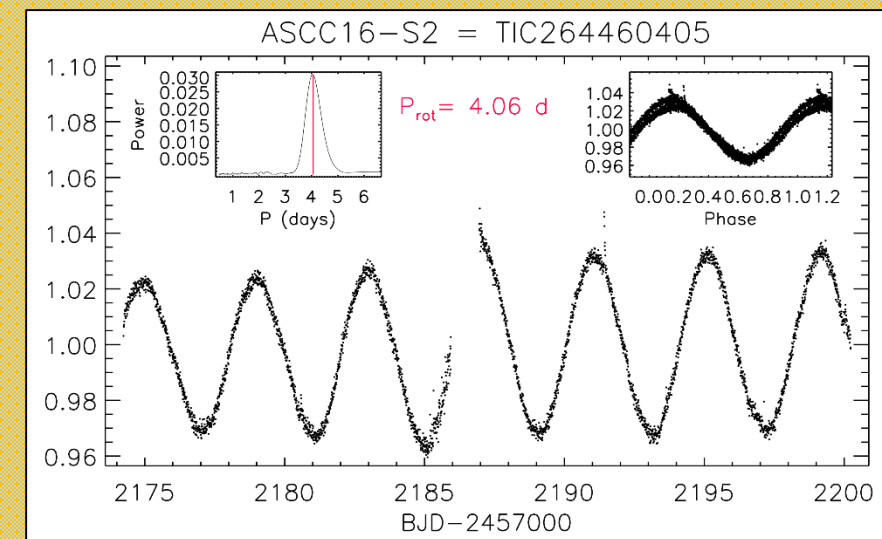
- Few representative stars per cluster → Observation time optimization
- (Moderately) slow rotators → Main Sequence G-type stars



Mamajek calibration

$$V_{\text{broad}} < 40 \text{ km/s}$$

$$\text{Prot} \geq 3 \text{ d (TESS)}$$



DATA COLLECTION

26 – 28 October, 2022



3.6-m Telescopio Nazionale Galileo

GIARPS

Claudi et al. 2017

HARPS-N

Cosentino et al. 2014

R = 115 000
3900 – 6800 Å

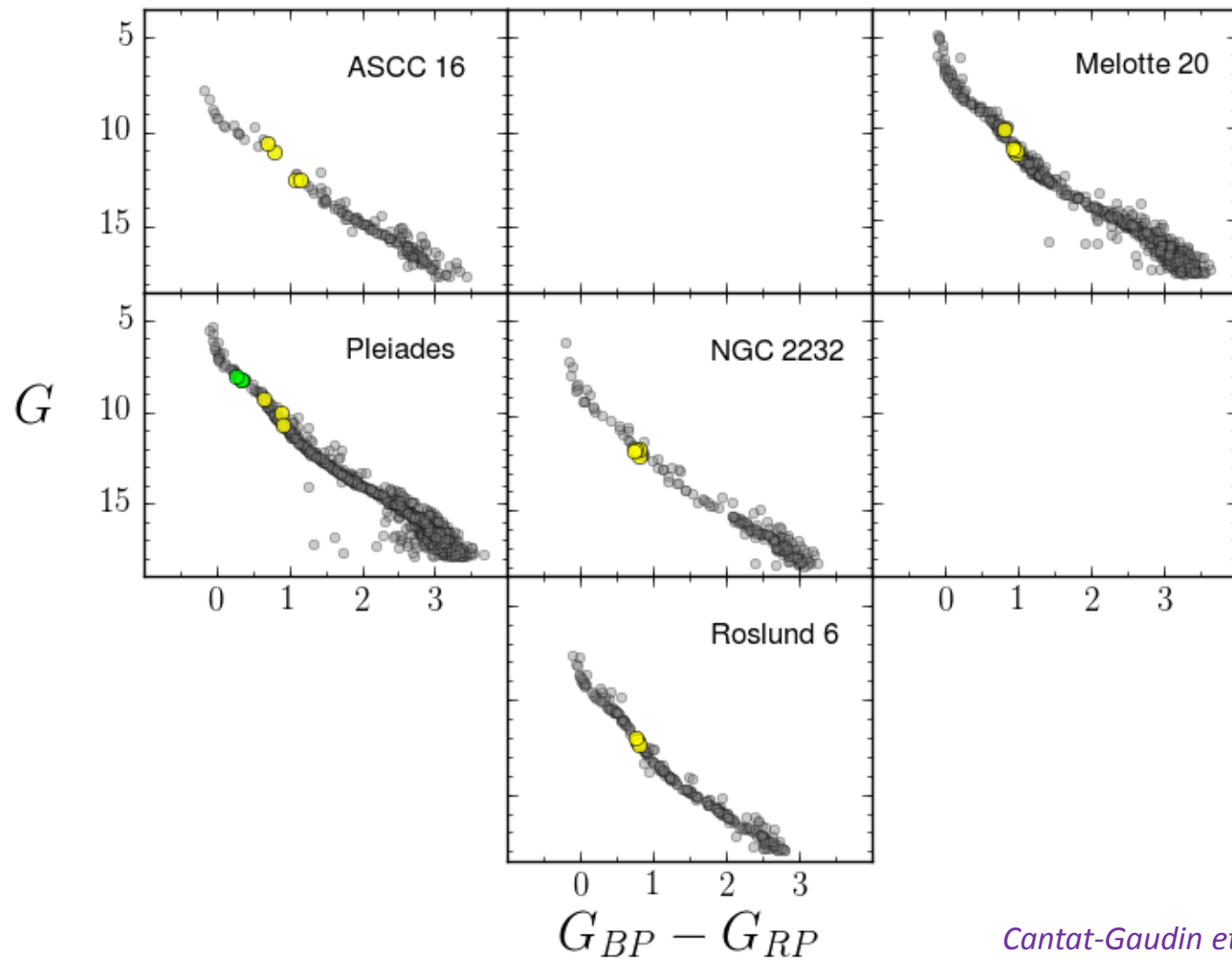


GIANO-B

Oliva et al. 2012, Origlia et al 2014

R = 55 000
9700 – 24 500 Å

DATA COLLECTION



Cantat-Gaudin et al. 2020

Cluster	Obs
---------	-----

ASCC 16:	4
----------	---

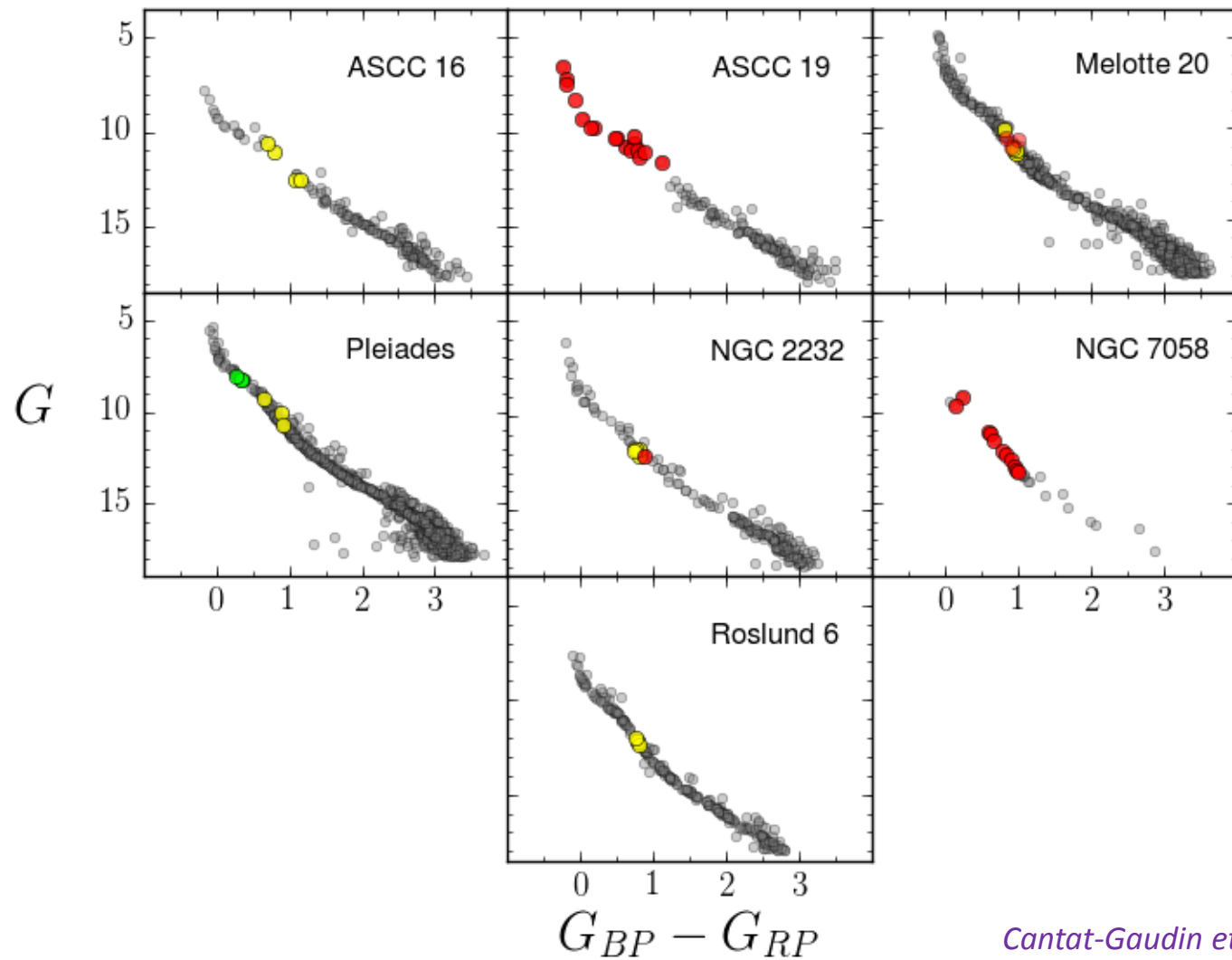
Melotte 20:	5
-------------	---

Pleiades:	3 (+3)
-----------	--------

NGC 2232:	4
-----------	---

Roslund 6:	4
------------	---

DATA COLLECTION



Cantat-Gaudin et al. 2020

Cluster	Obs	SPA
ASCC 16:	4	
ASCC 19:		17
Melotte 20:	5	3
Pleiades:	3 (+3)	
NGC 2232:	4	2
NGC 7058:		12
Roslund 6:	4	

DATA COLLECTION

Clusters main parameters

Cluster	$r50$ ($^{\circ}$)	N	$\log \tau$	A_V	d (pc)
ASCC 16	0.376	175	7.13	0.20	344
ASCC 19	0.605	149	7.02	0.13	346
Melotte 20	2.027	747	7.71	0.30	171
Pleiades	1.274	952	7.89	0.18	128
NGC 2232	0.516	188	7.25	0.01	315
NGC 7058	0.109	26	7.61	0.18	350
Roslund 6	1.004	247	7.95	0.00	375

Cantat-Gaudin et al. 2020

Stars observed

4

17

8

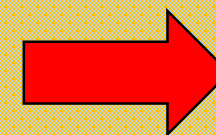
6

6

12

4

Total number of stars in our sample
(2019 – 2022)



57

RESULTS

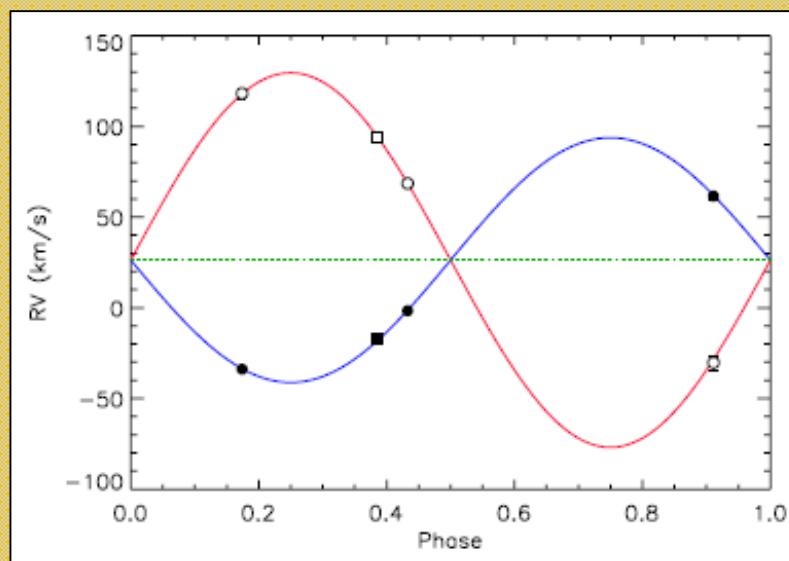
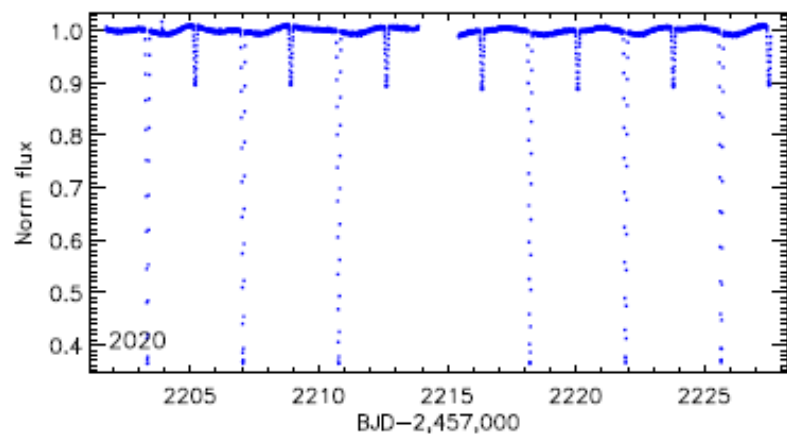
A&A 677, A154 (2023)

<https://doi.org/10.1051/0004-6361/202347226>

© The Authors 2023

Astronomy
&
Astrophysics

TIC 43152097 The first eclipsing binary in NGC 2232★

A. Frasca¹, J. Alonso-Santiago¹, G. Catanzaro¹, A. Bragaglia², V. D'Orazi^{3,4}, X. Fu^{5,2},
A. Vallenari⁴, and G. Andreuzzi^{6,7}

Orbital parameters

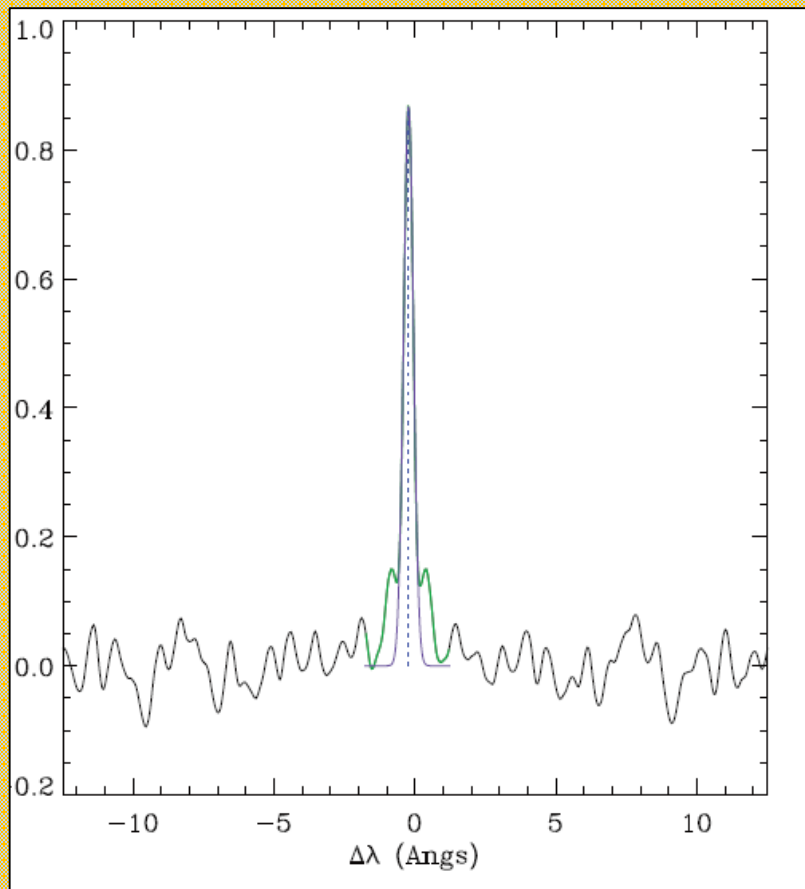
$BJD_0^{(a)}$	2225.641 ± 0.001
$P_{\text{orb}} \text{ (d)}$	3.718265 ± 0.000007
e	0
$\omega \text{ (}^\circ\text{)}$...
$\gamma \text{ (km s}^{-1}\text{)}$	26.27 ± 0.58
$K_1 \text{ (km s}^{-1}\text{)}$	67.48 ± 0.78
$K_2 \text{ (km s}^{-1}\text{)}$	103.28 ± 3.32
$M_1 \sin^3 i \text{ (}M_\odot\text{)}$	1.160 ± 0.083
$M_2 \sin^3 i \text{ (}M_\odot\text{)}$	0.758 ± 0.033
$q = M_2/M_1$	0.653 ± 0.022
$a \sin i \text{ (}R_\odot\text{)}$	12.54 ± 0.25

Stellar parameters

$M_1 \text{ (}M_\odot\text{)}$	1.160 ± 0.083
$M_2 \text{ (}M_\odot\text{)}$	0.758 ± 0.033
$R_1 \text{ (}R_\odot\text{)}$	1.121 ± 0.022
$R_2 \text{ (}R_\odot\text{)}$	0.885 ± 0.021
$\log g_1 \text{ (cgs)}$	4.423 ± 0.020
$\log g_2 \text{ (cgs)}$	4.440 ± 0.016
$T_1 \text{ (K)}$	6070 ± 70
$T_2 \text{ (K)}$	4130 ± 60
$L_1 \text{ (}L_\odot\text{)}$	1.531 ± 0.093
$L_2 \text{ (}L_\odot\text{)}$	0.204 ± 0.015

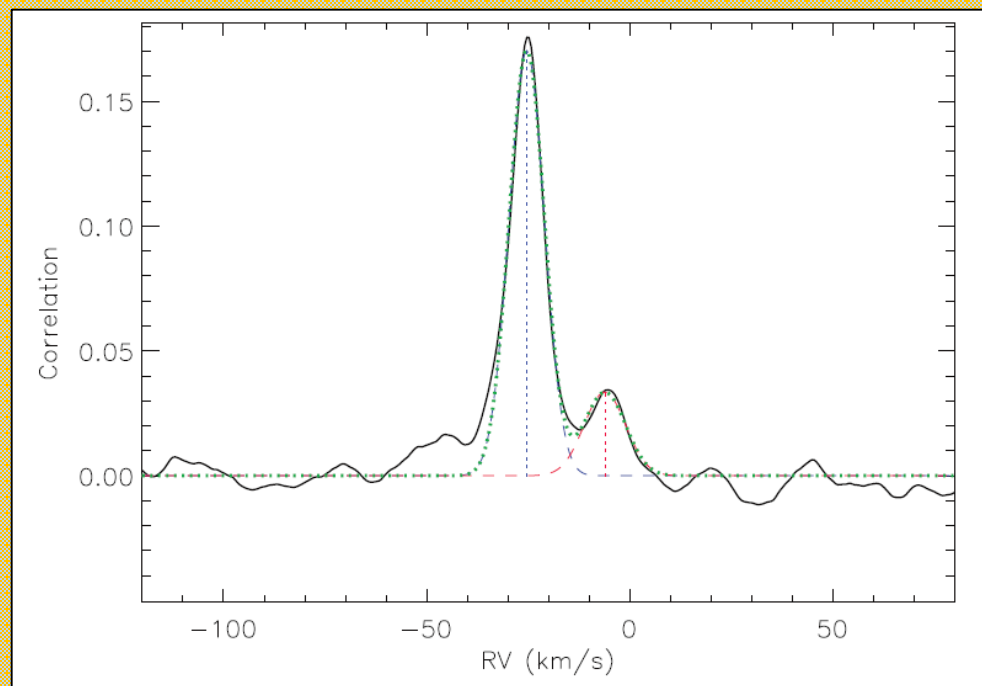
RESULTS

Radial velocity



Single

Different CCFs



SB2

RESULTS

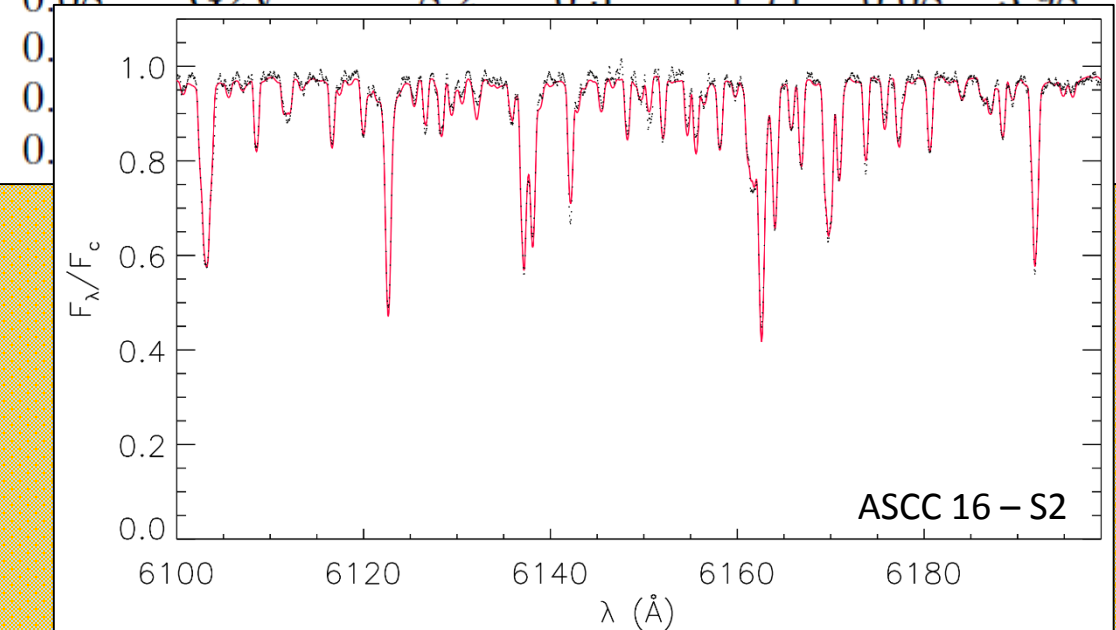
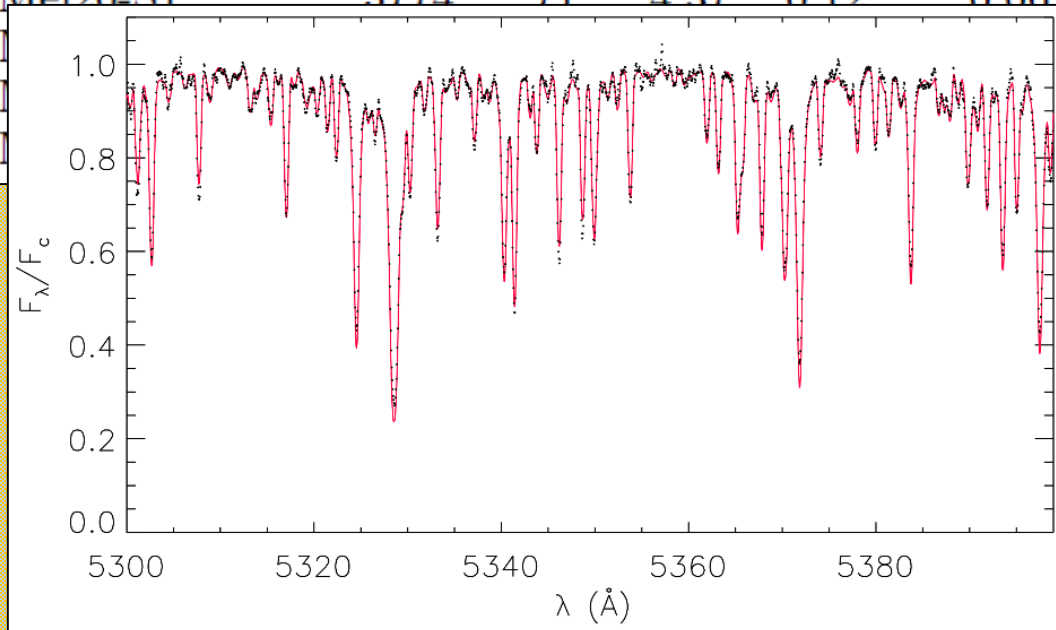
Stellar Parameters

Single FGK stars (41)

ROTFIT

Frasca et al. 2021

ID	T_{eff} (K)	err	$\log g$ (dex)	err	[Fe/H] (dex)	err	SpT	$v \sin i$ (km s^{-1})	err	RV (km s^{-1})	err	P_{rot}^a (d)
Mel20-A1	5752	69	4.35	0.12	0.19	0.07	G2.5V	1.9	1.4	-5.98	0.07	...
Mel20-A2	5843	71	4.44	0.11	-0.03	0.10	G1V	11.6	0.4	-1.62	0.12	4.08
Mel20-A3	6101	70	4.20	0.10	0.09	0.08	F8V	4.4	0.8	-0.68	0.06	2.64
Mel20-S1	5774	71	4.37	0.12	0.06	0.08	G2V	8.2	0.5	1.71	0.08	3.98



RESULTS

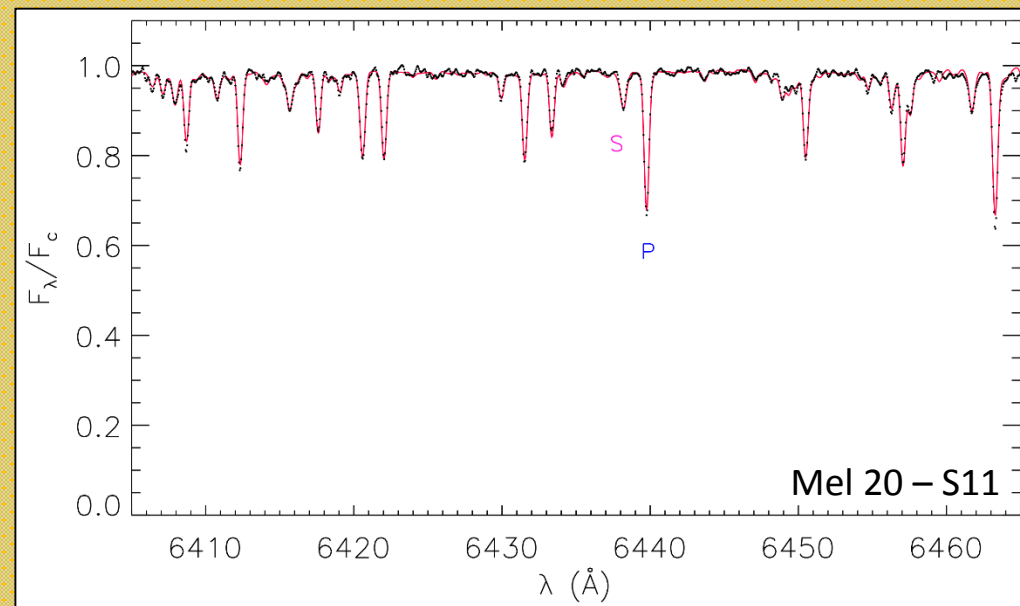
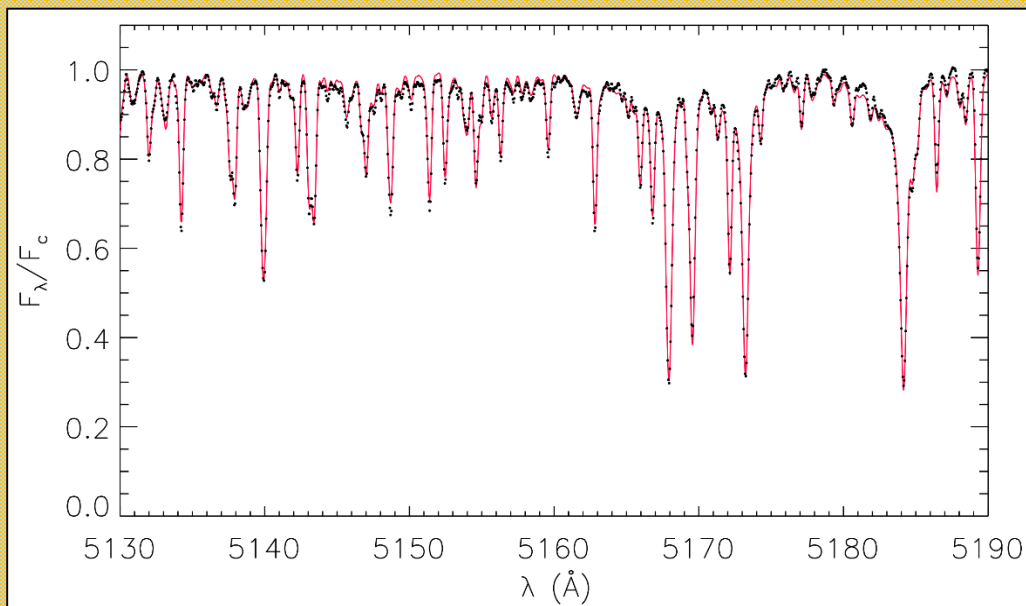
Stellar Parameters

COMPO2

Frasca et al. 2021

SB2 FGK stars (3)

ID	T_{eff} (K) [P/S]	err (K) [P/S]	$\log g$ (dex) [P/S]	err (dex) [P/S]	RV (km s^{-1}) [P/S]	err [P/S]	γ (km s^{-1})	w_{4400}^P	w_{5500}^P	w_{6400}^P	SpT [P/S]	$v \sin i$ (km s^{-1}) [P/S]
Mel20-S11	6119/5172	75/240	4.02/3.92	0.14/0.62	31.74/-41.46	0.15/2.39	4.2 ± 1.2	0.91 ± 0.02	0.89 ± 0.02	0.90 ± 0.03	F7IV/K1IV	8/8
Plei-S2	5674/5371	139/172	4.36/4.39	0.13/0.14	14.32/0.20	0.22/0.30	7.4 ± 0.2^a	0.56 ± 0.03	0.55 ± 0.03	0.53 ± 0.03	G2V/G2V	4/3
ASCC19-S7	5376/4894	139/226	4.41/4.36	0.11/0.40	35.49/9.11	0.25/1.16	24.6 ± 0.5	0.87 ± 0.02	0.83 ± 0.02	0.79 ± 0.04	G8V/K4V	7/7



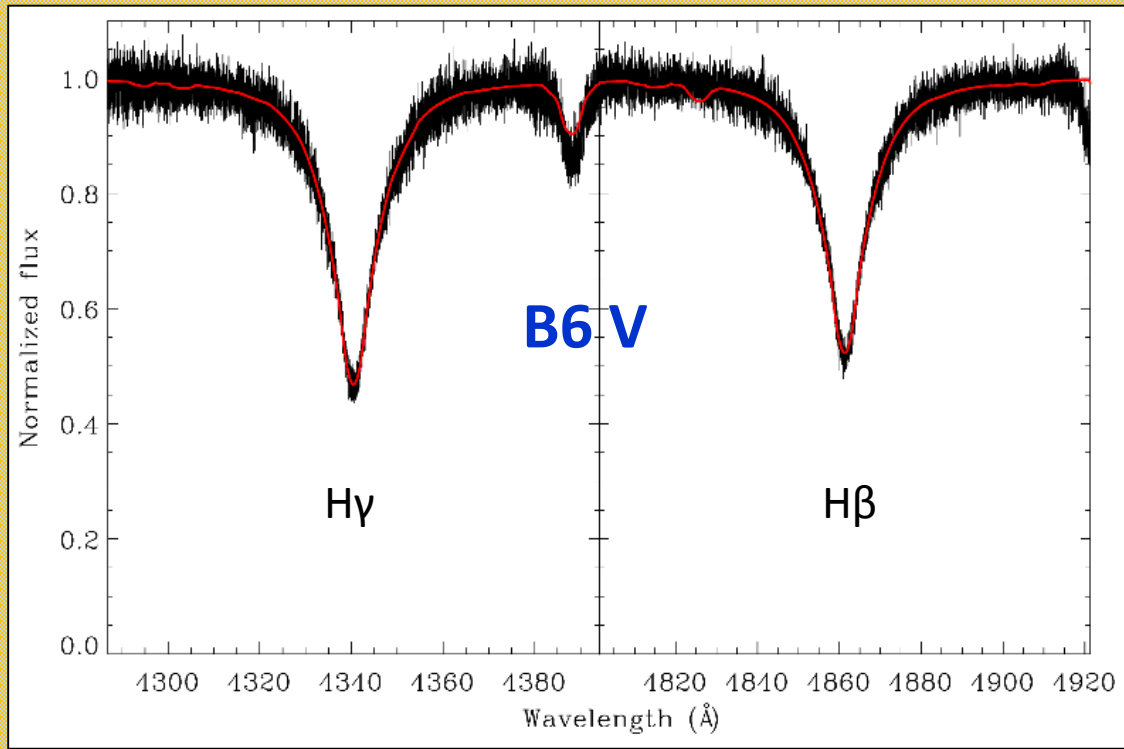
RESULTS

Stellar Parameters

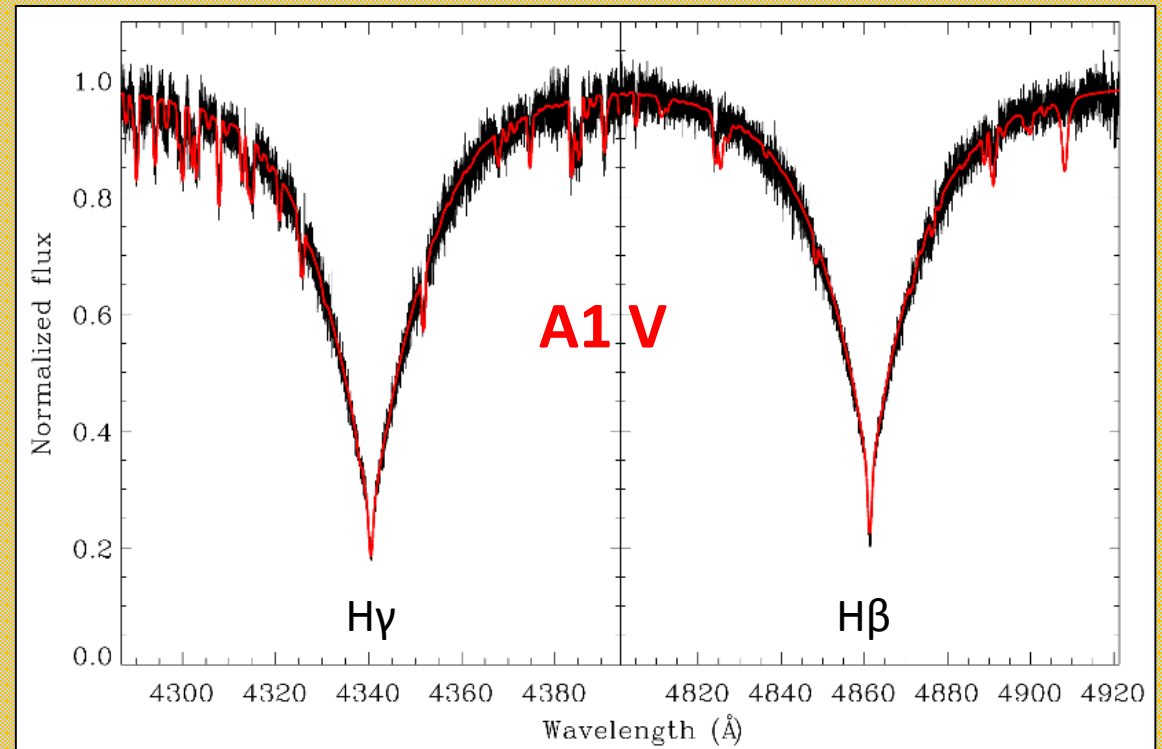
Single hot stars (12)



Spectral synthesis of the Balmer lines



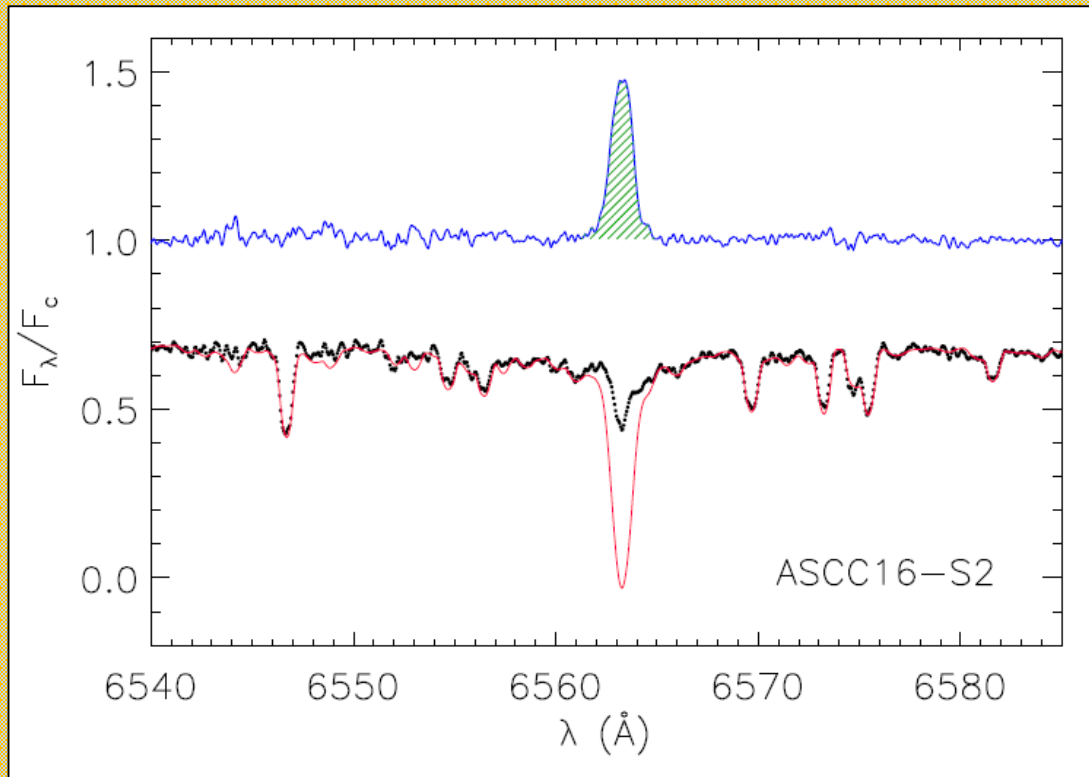
ASCC 19 - S19



ASCC 19 - S21

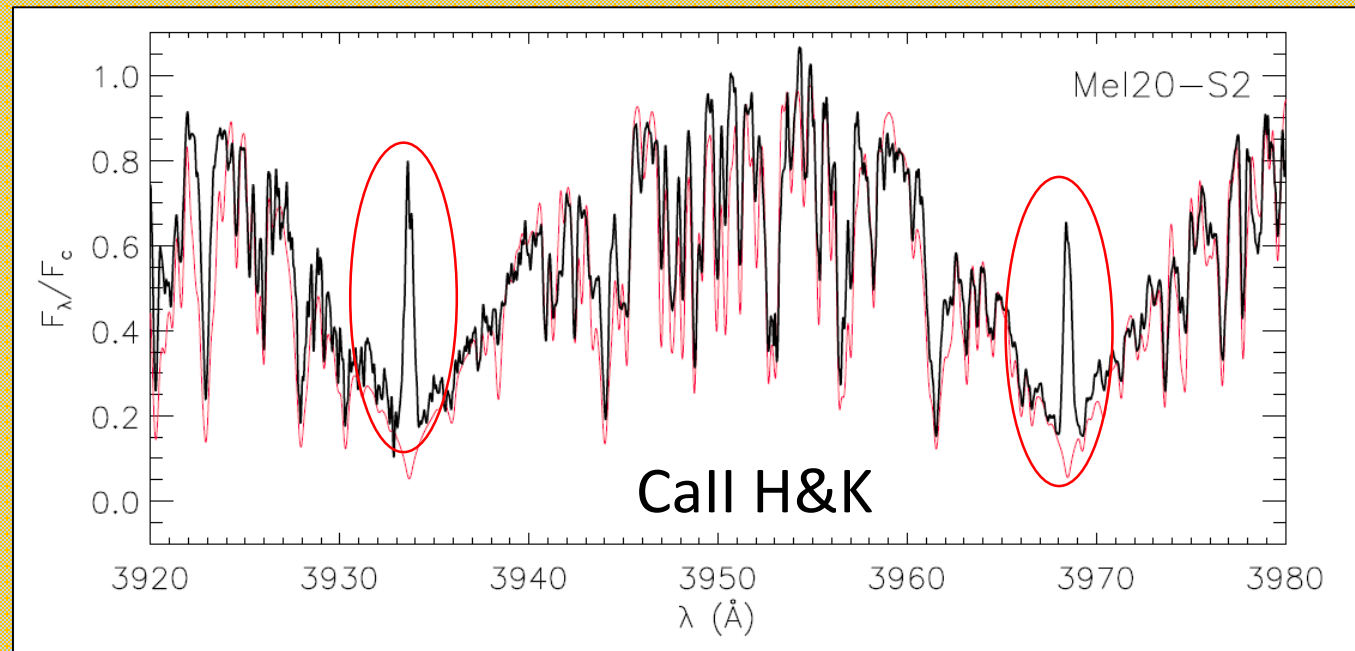
RESULTS

Chromospheric activity

H α

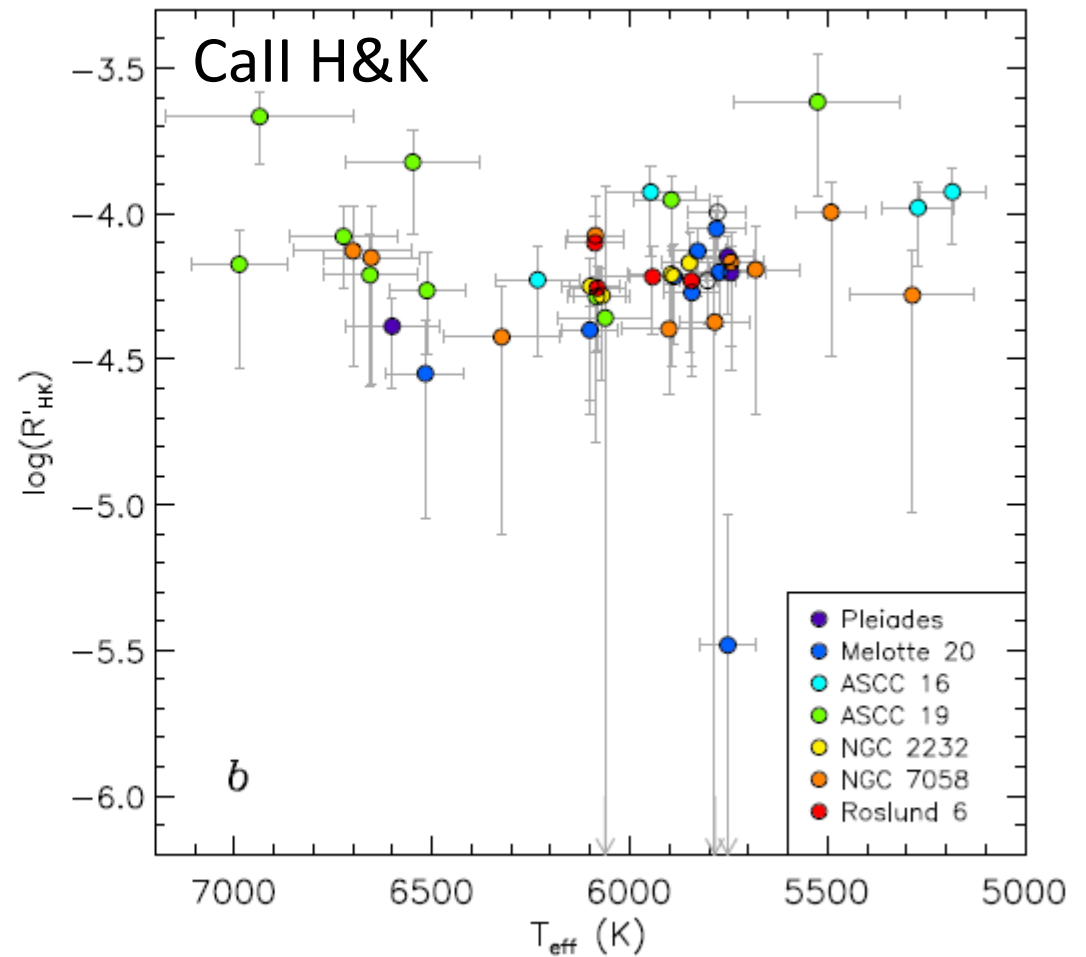
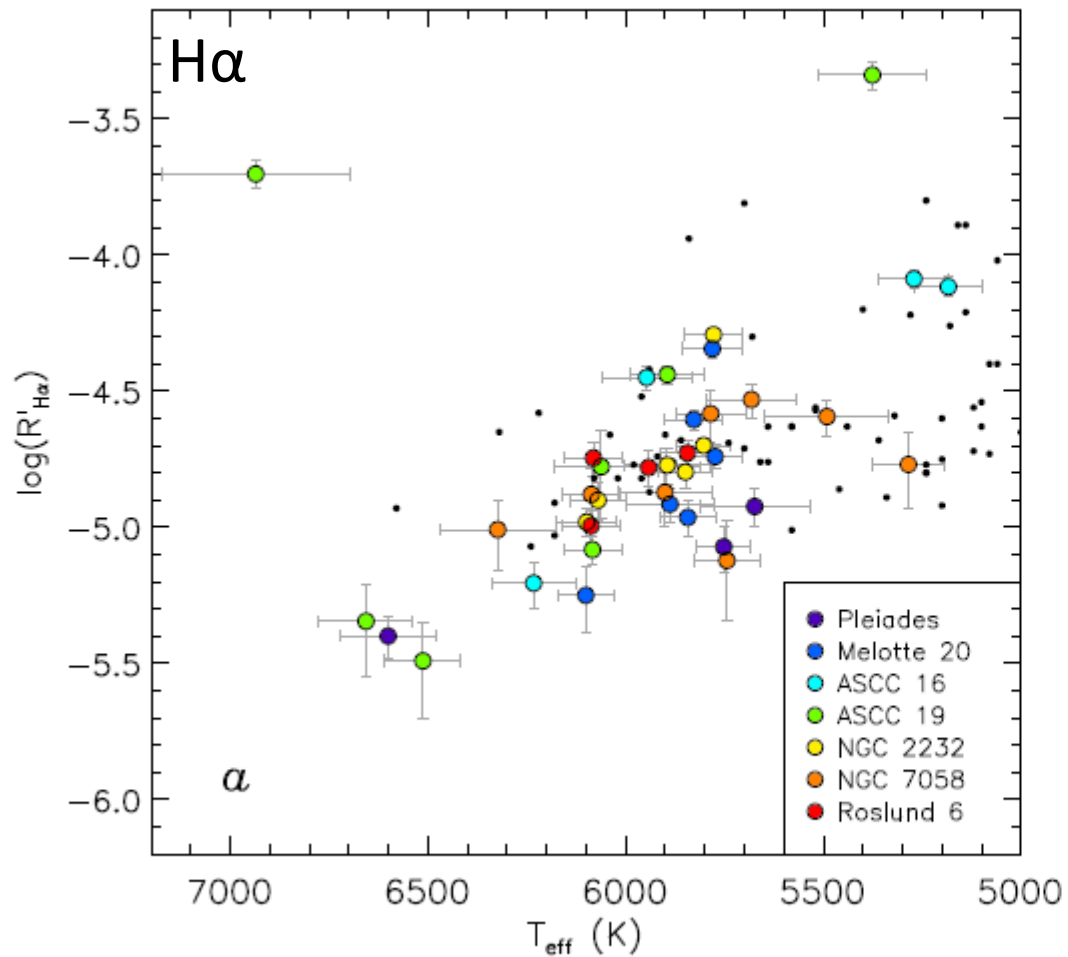
$$F_{\text{H}\alpha} = F_{6563} EW_{\text{H}\alpha},$$

$$R'_{\text{H}\alpha} = L_{\text{H}\alpha}/L_{\text{bol}} = F_{\text{H}\alpha}/(\sigma T_{\text{eff}}^4)$$



RESULTS

Chromospheric activity

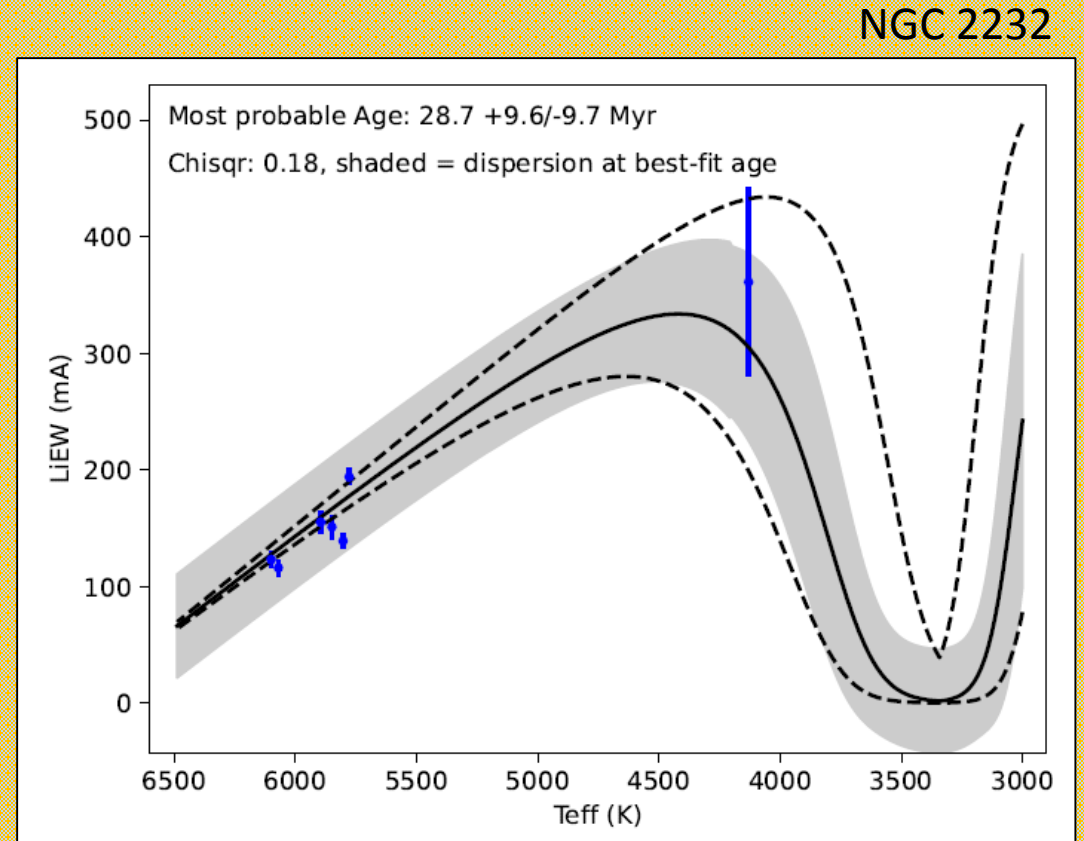


RESULTS

Li Abundance and Age

Cluster	CG20	This work
ASCC 16	13	14±10
ASCC 19	10	<20
Melotte 20	51	68±28
Pleiades	78	75±36
NGC 2232	18	29±10
NGC 7058	41	65±23
Roslund 6	89	108±66

Compatible results:
isochrone-fitting vs Li depletion



EAGLES *Jeffries et al. 2023*

RESULTS

Chemical abundances

Spectral synthesis

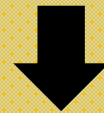
FGK Stars

Catanzaro 2011,2013

1D LTE Models

ATLAS9

Kurucz 1993a,b



Synthetic spectra

Observed spectra

SYNTHE

Kurucz & Avrett 1981

39 spectral segments of 50 Å
(4400 – 6800 Å)

χ^2 - minimization

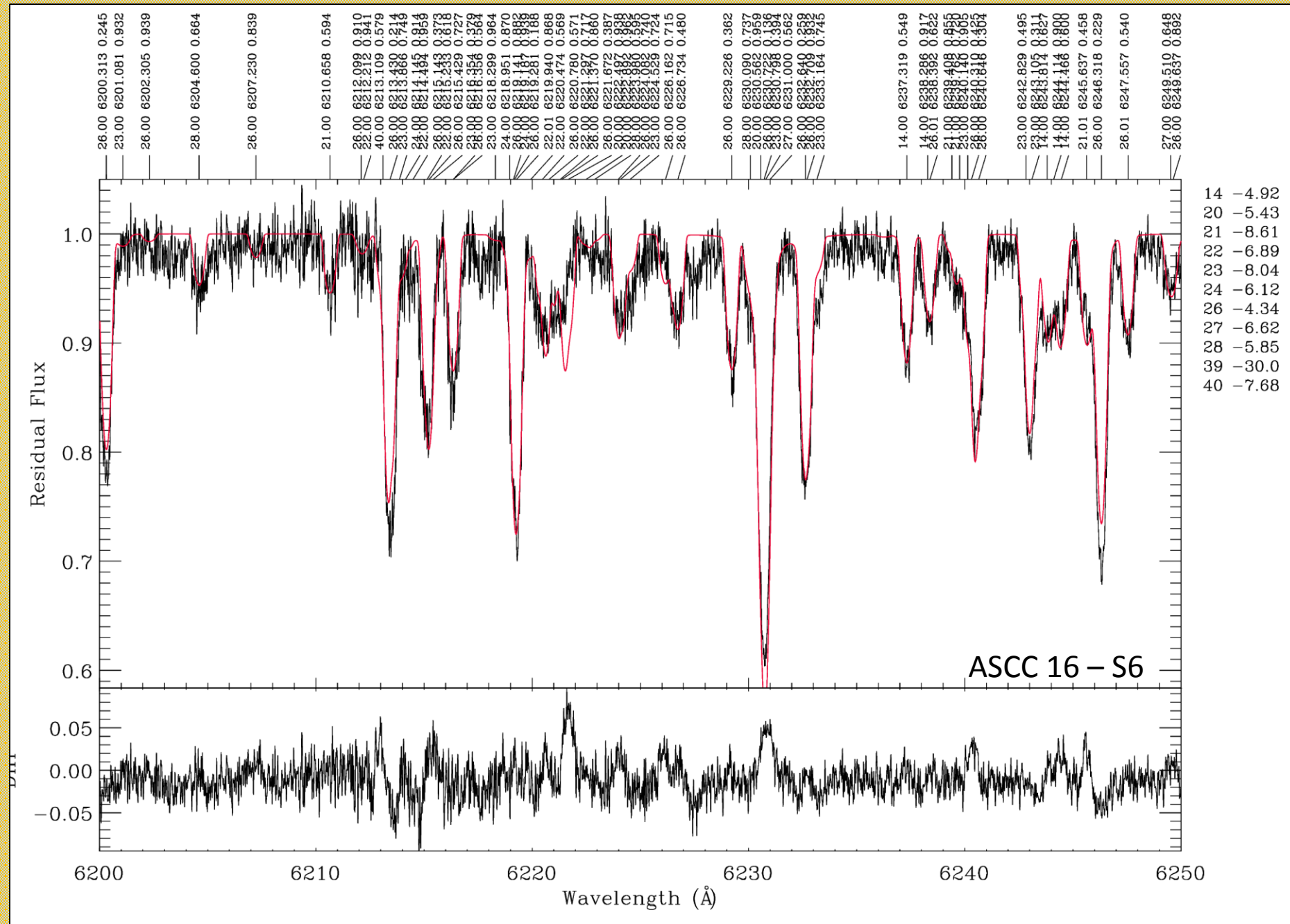
$A(X)$

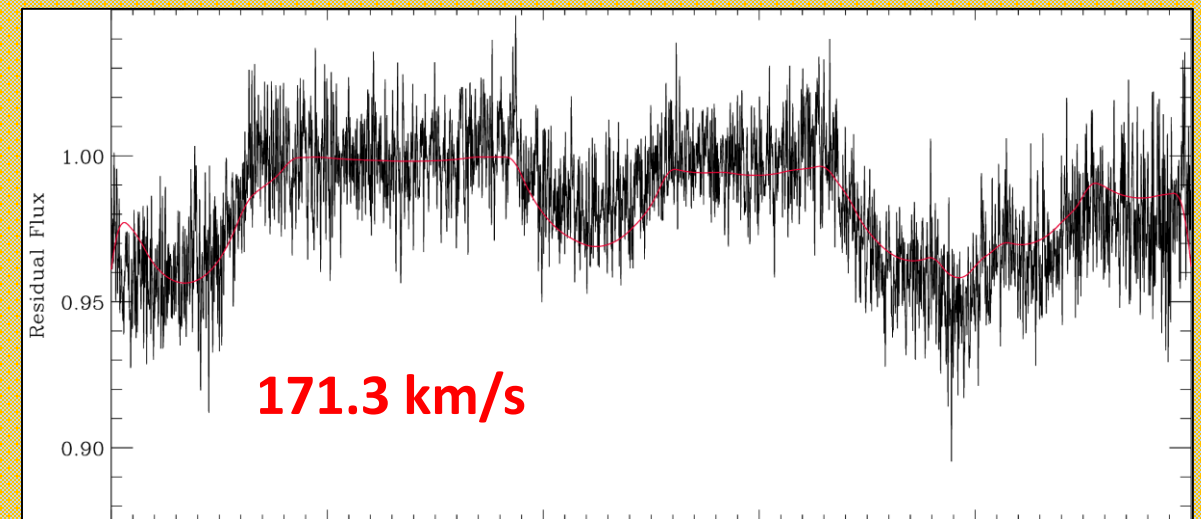
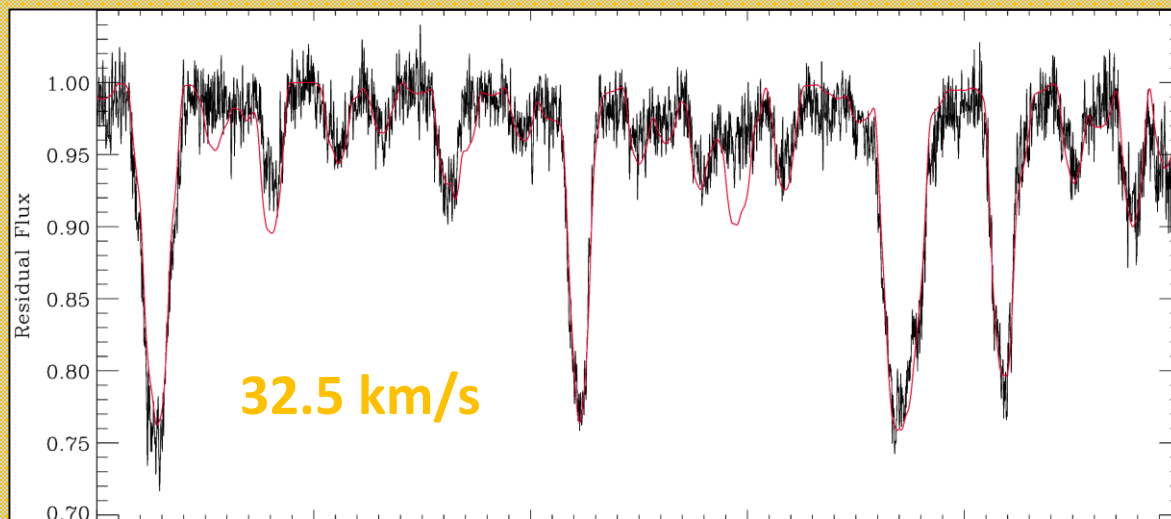
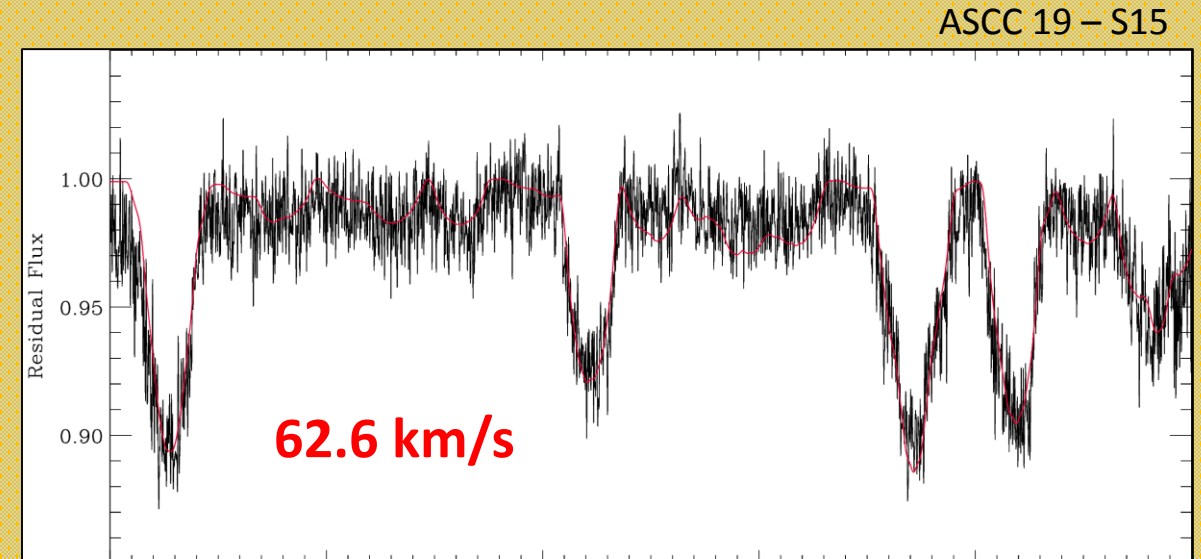
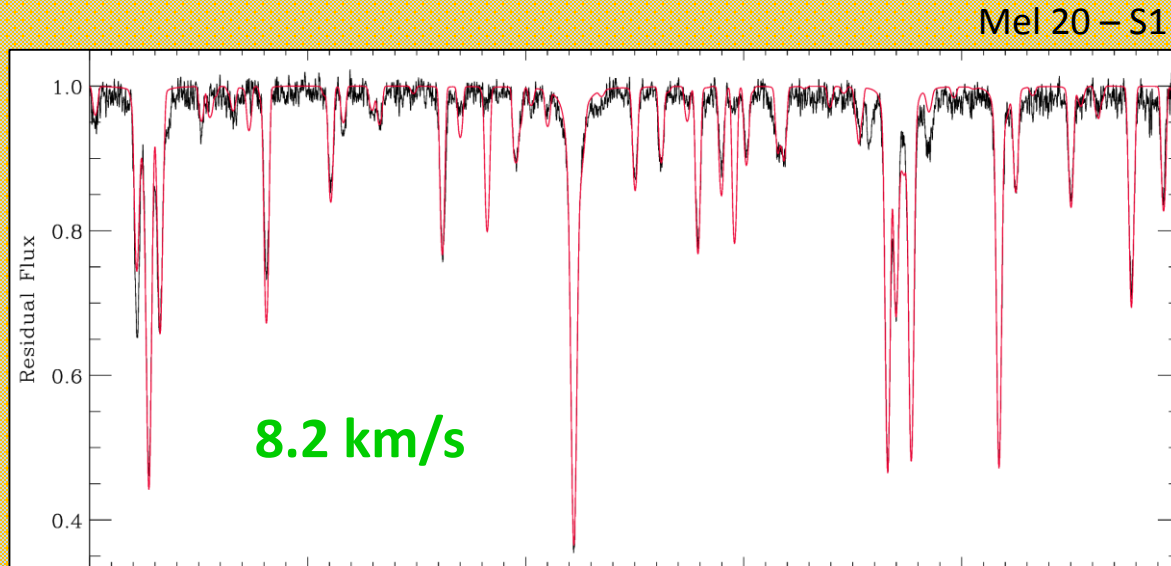
Procedure overview

RESULTS

Chemical abundances

Example of fitting



RESULTS**Effect of $v \sin i$ on the spectrum**

ASCC 16 – S6

ASCC 19 – S2

RESULTS

Preliminary !!

Chemical
abundances

[X/H]

Grevesse et al. 2007

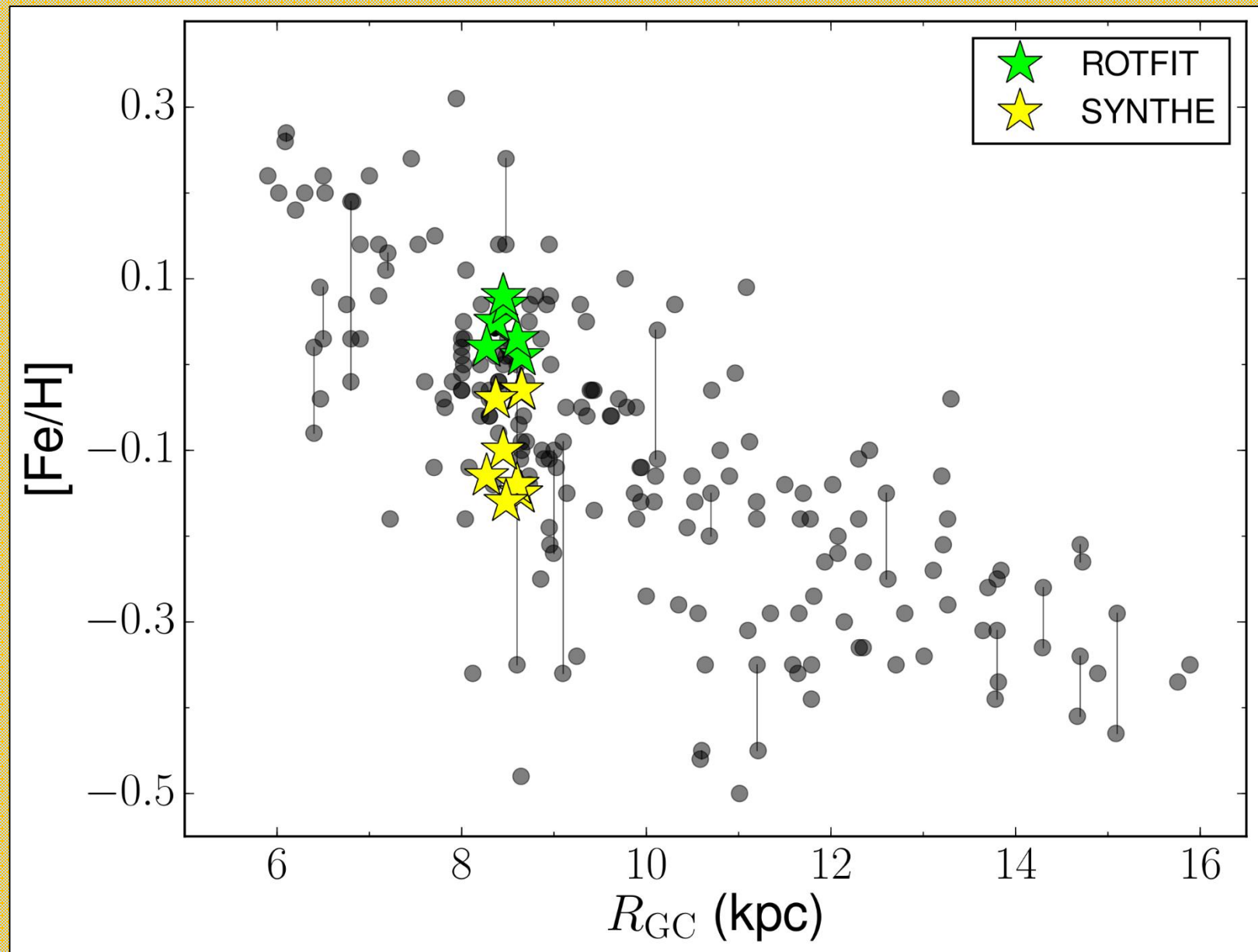
X	Melotte 20	Pleiades	ASCC 16	ASCC 19	NGC 2232	Roslund 6	NGC 7058
C	0.35±0.08	0.21±0.12	0.34±0.15	0.23±0.08	0.38±0.06	0.38±0.04	0.10±0.18
Na	0.06±0.14	0.07±0.07	0.06±0.09	0.03±0.18	-0.01±0.05	0.04±0.05	0.12±0.11
Mg	-0.04±0.07	0.06±0.06	0.02±0.06	-0.07±0.12	-0.01±0.01	0.00±0.04	0.04±0.16
Al	0.18±0.18	0.19±0.01	0.22±0.12	0.19±0.08	0.12±0.07	0.11±0.09	0.13±0.08
Si	-0.15±0.07	-0.05±0.14	-0.03±0.05	-0.01±0.10	-0.12±0.07	-0.08±0.09	-0.08±0.09
S	0.23±0.20	0.16±0.16	0.27±0.08	0.16±0.06	0.29±0.12	0.24±0.12	0.33±0.11
Ca	0.10±0.08	0.13±0.13	0.11±0.06	0.03±0.08	0.13±0.06	0.17±0.06	0.14±0.12
Sc	-0.05±0.07	0.01±0.08	0.19±0.06	-0.11±0.07	-0.03±0.10	-0.04±0.07	0.06±0.07
Ti	-0.05±0.10	0.08±0.11	0.13±0.09	-0.02±0.11	0.00±0.08	-0.04±0.06	0.06±0.10
V	0.10±0.06	0.20±0.11	0.19±0.10	0.21±0.05	0.16±0.04	0.13±0.04	0.14±0.07
Cr	0.01±0.10	0.09±0.14	0.11±0.11	0.05±0.11	0.05±0.09	0.05±0.08	0.08±0.11
Mn	0.08±0.09	0.15±0.14	0.13±0.09	-0.01±0.08	0.09±0.07	0.10±0.05	0.12±0.09
Fe	-0.16±0.16	-0.10±0.24	-0.03±0.12	-0.15±0.17	-0.14±0.12	-0.13±0.09	-0.04±0.12
Co	0.12±0.08	0.18±0.05	0.18±0.04	0.20±0.05	0.13±0.05	0.17±0.02	0.16±0.08
Ni	-0.10±0.07	-0.01±0.04	0.01±0.09	-0.07±0.12	-0.09±0.06	-0.06±0.09	0.02±0.05
Cu	-0.02±0.12	-0.10±0.23	0.01±0.15	-0.14±0.17	0.01±0.16	-0.13±0.08	-0.06±0.14
Zn	-0.26±0.10	-0.34±0.20	-0.23±0.12	-0.27±0.12	-0.26±0.07	-0.26±0.08	-0.21±0.14
Sr	0.20±0.09	0.07±0.11	0.26±0.15	0.15±0.14	0.08±0.07	0.17±0.07	0.17±0.13
Y	0.20±0.09	0.22±0.13	0.23±0.13	0.14±0.09	0.21±0.07	0.18±0.08	0.13±0.09
Zr	0.13±0.04	0.23±0.05	0.17±0.12	0.15±0.08	0.14±0.03	0.11±0.04	0.14±0.05
Ba	0.15±0.31	-0.03±0.06	0.08±0.18	0.24±0.12	0.45±0.07	0.36±0.07	0.34±0.13
La	0.26±0.10	0.32±0.07	0.22±0.11	0.27±0.10	0.27±0.05	0.28±0.06	0.25±0.11
Ce	0.14±0.09	0.17±0.02	0.15±0.13	0.12±0.08	0.19±0.04	0.12±0.06	0.23±0.15

RESULTS

Chemical abundances

Galactic gradient

HR spectroscopy of OCs
(APOGEE, SPA, GES)

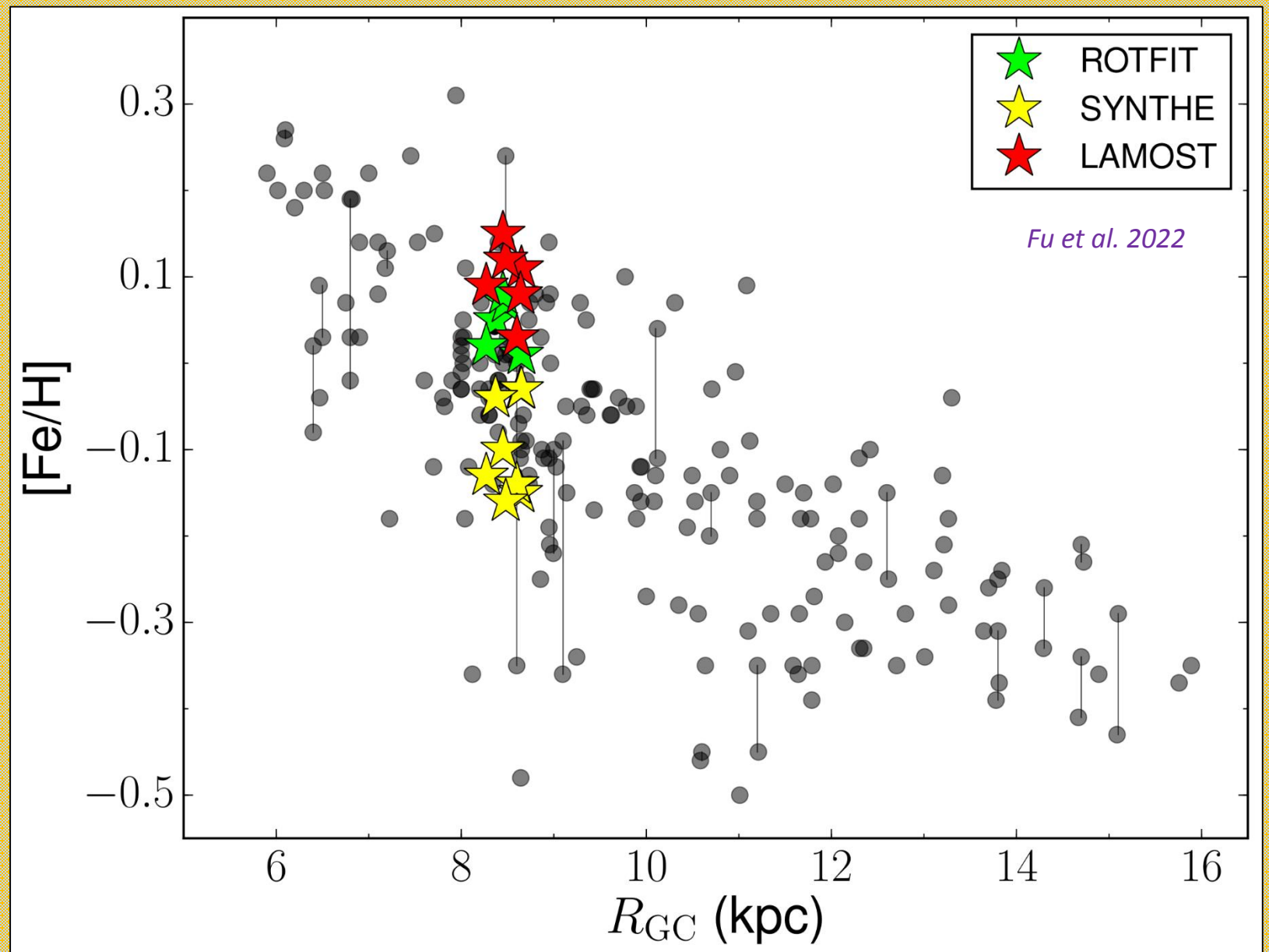


RESULTS

Chemical
abundances

Galactic gradient

HR spectroscopy of OCs
(APOGEE, SPA, GES)

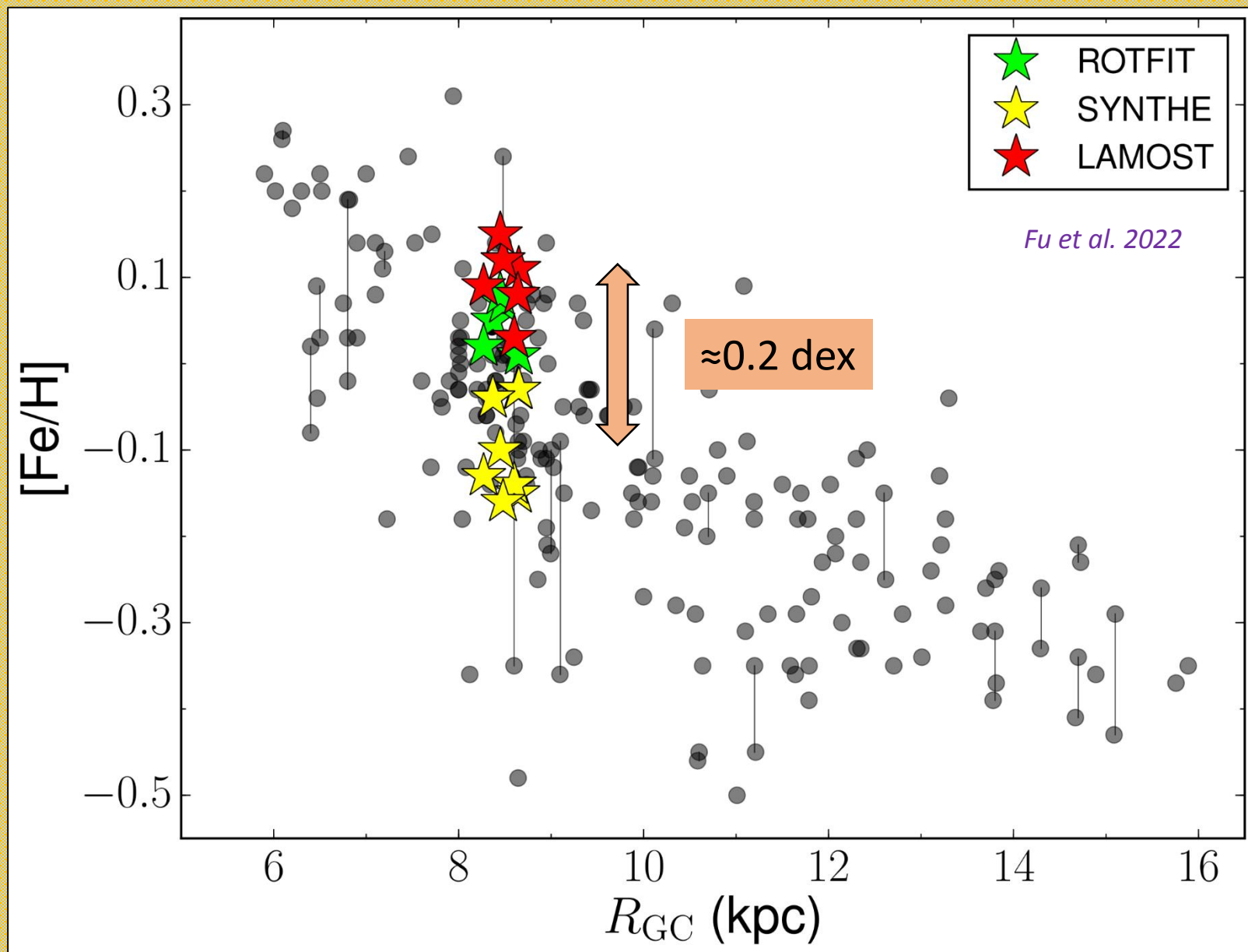


RESULTS

Chemical abundances

Galactic gradient

HR spectroscopy of OCs
(APOGEE, SPA, GES)



RESULTS

Chemical abundances

Grevesse et al. 2007

Galactic trends

HR spectroscopy of OCs
(APOGEE, SPA, GES)

